

Distribution Agreement

In presenting this thesis as a partial fulfillment of the requirements for a degree from Emory University, I hereby grant to Emory University and its agents the non-exclusive license to archive, make accessible, and display my thesis in whole or in part in all forms of media, now or hereafter now, including display on the World Wide Web. I understand that I may select some access restrictions as part of the online submission of this thesis. I retain all ownership rights to the copyright of the thesis. I also retain the right to use in future works (such as articles or books) all or part of this thesis.

Jocelyn Lee

March 28, 2025

Targeting EP300/CBP to Overcome IMiD Resistance in Multiple Myeloma

by

Jocelyn Lee

Benjamin Barwick, PhD

Adviser

Center for the Study of Human Health

Benjamin Barwick, PhD

Adviser

Vikas Gupta, MD, PhD

Committee Member

Amanda Freeman, PhD

Committee Member

2025

Targeting EP300/CBP to Overcome IMiD Resistance in Multiple Myeloma

by

Jocelyn Lee

Benjamin Barwick, PhD

Adviser

An abstract of

a thesis submitted to the Faculty of Emory College of Arts and Sciences

of Emory University in partial fulfillment

of the requirements of the degree of

Bachelor of Arts with Honors

Center for the Study of Human Health

2025

Abstract

Targeting EP300/CBP to Overcome IMiD Resistance in Multiple Myeloma

By Jocelyn Lee

Multiple Myeloma is a blood cancer of plasma cells in the bone marrow. Immunomodulatory drugs (IMiDs) are a backbone therapy used for myeloma. IMiDs bind the ubiquitin-ligase Cereblon and redirect it to the transcription factors Ikaros (IKZF1) and Aiolos (IKZF3), targeting them for proteasomal degradation. This corresponds with the downregulation of proto-oncogenes such as *MYC* and *IRF4*, which leads to myeloma cell death.

While IMiDs initially work well, most myeloma patients become IMiD-resistant. Several studies have suggested mechanisms of resistance to IMiDs, including mutations in Cereblon, but these mutations only occur in some patients. Other studies have identified that transcription factors (ETV4, BATF, BATF2, and BATF3) can maintain *MYC* and *IRF4* expression independently of IKZF1/IKZF3, allowing myeloma to proliferate.

EP300 and CBP are transcriptional co-activators that catalyze the acetylation of histones necessary for *MYC* and *IRF4* expression. Targeting EP300 and CBP has recently been considered an approach to overcoming IMiD resistance. CCS1477 is an EP300/CBP inhibitor in Phase 2 clinical trials and has seen overall response rates of ~70% in myeloma patients, including IMiD-resistant cases. Previous studies have used other EP300/CBP inhibitors in combination with IMiDs and found that the combination downregulated *MYC* and *IRF4* and cell viability. We aim to determine if there is synergy between CCS1477 and the IMiD pomalidomide.

Experiments using varying doses of CCS1477 and pomalidomide in combination and separately were conducted on both IMiD-sensitive and IMiD-resistant cell lines. Combined EP300/CBP inhibition and pomalidomide decreased *MYC* expression in myeloma cell models. All cell lines had a dose-dependent decrease in viability when CCS1477 and pomalidomide were combined. There was therapeutic synergy in H929 and MM1S across all combination doses and in RPMI8226 and JJN3 at the highest combination doses.

Our results show therapeutic potential for using CCS1477 and pomalidomide in combination to downregulate important oncogenes such as *MYC*. There was therapeutic synergy in both IMiD-resistant and sensitive cell lines. While there is still much more to understand about the mechanism of synergy between IMiDs and

EP300/CBP inhibitors, the combination of CCS1477 and pomalidomide has promising therapeutic uses for myeloma patients.

Targeting EP300/CBP to Overcome IMiD Resistance in Multiple Myeloma

by

Jocelyn Lee

Benjamin Barwick, PhD

Adviser

A thesis submitted to the Faculty of Emory College of Arts and Sciences
of Emory University in partial fulfillment
of the requirements of the degree of
Bachelor of Arts with Honors

Center for the Study of Human Health

2025

Acknowledgements

I would like to thank Dr. Benjamin Barwick for his mentorship and support over the past two years. I could not have done this without his expertise, encouragement, and guidance, which have been instrumental in shaping both this project and my growth as a student and researcher.

I would like to thank Jonathan Patton for his guidance and efforts in assisting me through these experiments and with FlowJo analysis. Your help has been a vital part of my learning and scientific growth.

I would like to thank all of the members of the Barwick and Gupta Labs: Jonathan Patton, Kiran Lakhani, Robert Chavez, Doris Powell, and Hannah Barge. Special thanks to Dr. Beena E. Thomas and Dr. Lawrence Boise. I could not have done this without all of your continuous support throughout my time in the Barwick Lab.

I would like to thank Dr. Vikas Gupta and Dr. Amanda Freeman for their scientific expertise and time to serve on my committee.

Lastly, I would like to thank my family and friends. Your endless love and support have helped to push me through this project and other endeavors.

Table of Contents

INTRODUCTION	1
BACKGROUND ON MULTIPLE MYELOMA	1
THERAPEUTIC TARGETING OF MULTIPLE MYELOMA	2
IMMUNOMODULATORY DRUG RESISTANCE	4
TARGETING TRANSCRIPTIONAL CO-ACTIVATORS	5
RESEARCH AIMS.....	7
METHODS	11
CELL LINES	11
SAMPLE PREPARATION.....	11
SERIAL DILUTION OF CCS1477.....	11
SERIAL DILUTION OF POMALIDOMIDE	12
ANNEXIN V AND LIVE/DEAD STAINING AND DATA COLLECTION	12
DATA ANALYSIS	14
RESULTS.....	14
IMiD AND EP300/CBP INHIBITOR MODULATION OF <i>MYC</i> EXPRESSION AS MEASURED IN JJN3 D11	14
IMiD-RESISTANT CELL LINES	16
IMiD-SENSITIVE CELL LINES	18
RESULTS SUMMARY	20
DISCUSSION.....	28
OVERVIEW	28
RESULTS INTERPRETATION.....	29
THERAPEUTIC IMPLICATIONS.....	31
LIMITATIONS	32
FUTURE DIRECTIONS	33

CONCLUSION	34
REFERENCES.....	36

Table of Figures

FIGURE 1. MODEL OF IKZF1, IKZF3, EP300, CBP, AND OTHER TRANSCRIPTION FACTORS (TF) REGULATING <i>MYC</i> IN MULTIPLE MYELOMA	9
FIGURE 2. EP300 AND CBP ARE PARALOGOUS HISTONE ACETYLTRANSFERASES.	10
FIGURE 3A-B. IMiD AND EP300/CBP INHIBITOR MODULATION OF <i>MYC</i> EXPRESSION AS MEASURED IN JJN3 D11	22
FIGURE 4A-C. VIABILITY AND SYNERGY PLOTS FOR JJN3	23
FIGURE 5A-C. VIABILITY AND SYNERGY PLOTS FOR RPMI8226.....	24
FIGURE 6A-C. VIABILITY AND SYNERGY PLOTS FOR H929.....	25
FIGURE 7A-C. VIABILITY AND SYNERGY PLOTS FOR MM1S.....	26
FIGURE 8A-C. VIABILITY AND SYNERGY PLOTS FOR KMS26	27

Introduction

Background on Multiple Myeloma

Multiple Myeloma is a blood cancer of plasma cells in the bone marrow. Plasma cells are a type of B cell, which is part of the adaptive immune system that mounts antibody-based responses. Patients diagnosed with Multiple Myeloma often have hypercalcemia, renal failure, anemia, and/or lytic bone lesions, symptoms known as CRAB (Rajkumar, 2022). Multiple Myeloma is preceded by Monoclonal Gammopathy of Undetermined Significance (MGUS) and Smoldering Multiple Myeloma (SMM) (Kyle et al., 2018). MGUS is an asymptomatic stage that sometimes develops into SMM and Multiple Myeloma. MGUS and SMM patients do not have myeloma-defining symptomatic criteria – hypercalcemia, renal failure, anemia, and lytic bone lesions (CRAB). Once the patient's symptoms meet the diagnostic criteria of CRAB, they are considered to be in the Newly Diagnosed Multiple Myeloma (NDMM) stage. Relapsed Multiple Myeloma occurs when a patient's cancer stops responding to therapy and there is an expansion of Multiple Myeloma. Unfortunately, almost every patient eventually relapses (AJMC, 2022).

The initiating primary genetic events are present in MGUS and SMM and include hyperdiploidy, which is a trisomy of most odd-numbered chromosomes, and translocations of the Immunoglobulin Heavy (IgH) chain enhancer to a handful of oncogenes (Barwick et al., 2019). As the cancer progresses from MGUS/SMM to NDMM, secondary and tertiary genetic events occur. These events include translocations and structural variants that serve to amplify *MYC* expression, a proto-oncogene, and alterations in NF- κ B and Ras pathways that regulate cell growth (Misund et al., 2020). On

a genetic level, Newly Diagnosed Multiple Myeloma has over four hundred mutations per patient (Rajkumar, 2022). These include large genetic events such as deletions of chromosome 13q, 1p, and gains of chromosome 1q (Barwick et al., 2019)

Therapeutic Targeting of Multiple Myeloma

Current treatment options for Multiple Myeloma patients include proteasome inhibitors, Immunomodulatory Drugs (IMiDs) such as lenalidomide, CD38-targeting monoclonal antibodies (daratumumab), steroids (dexamethasone), and others. These drugs are typically used together in a triplet and quadruplet regimens, where the patient takes a combination of three or four drugs (Joseph et al., 2020). These initial treatments are referred to as induction therapy and are often followed by an autologous stem cell transplant. Induction therapy lasts about 5.5 months (Joseph et al., 2020). Patients receive maintenance therapy after receiving an autologous stem cell transplant (Joseph et al., 2020). The most common maintenance therapy is an immunomodulatory drug (IMiD). IMiDs are derivatives of thalidomide that target proteins leading to the inhibition of myeloma cell proliferation. Thalidomide was used to treat nausea in pregnant women but was found to cause birth defects. The most commonly used IMiDs in Multiple Myeloma management include: lenalidomide and pomalidomide (Joseph et al., 2020). IMiDs target the transcription factors Ikaros (IKZF1) and Aiolos (IKZF3), which are necessary for the development of B cells and plasma cells (Georgopoulos et al., 1992). In previous studies, myeloma cells treated with IMiDs lead to a decreased amount of IKZF1 and IKZF3 protein (Krönke et al., 2014). IMiDs work by binding Cereblon protein (CRBN), which is part of a ubiquitin ligase complex, and redirecting it to IKZF1 and IKZF3, which are subsequently ubiquitinated and targeted for degradation by the proteasome (Krönke et al., 2014). It was

also found that IMiDs stabilize CRBN, which allows for greater binding of IKZF1 and IKZF3 to CRBN (Lu et al., 2014).

Formative studies in Multiple Myeloma found growth was dependent upon *MYC* and *IRF4* (Shaffer et al., 2008). Subsequent studies have illustrated that when IMiD-sensitive Multiple Myeloma cells are treated with IMiDs, *MYC* and *IRF4* are downregulated along with depletion of IKZF1 and IKZF3 (**Fig. 1**) (Zhu et al., 2011). *MYC* is a very well-studied proto-oncogene that, when dysregulated, leads to rapid and uncontrollable growth, contributing to cancer development and progression. High expression of *MYC* has been linked to poor cancer prognosis (Steinberger et al., 2019). *IRF4* is a transcription factor responsible for regulating metabolic control, cell cycle progression, cell death (apoptosis), and transcriptional regulation. (Shaffer et al., 2008). The gene targets of *IRF4* regulate glucose metabolism pathways and ATP synthesis, which are critical for cell energy and survival. Previous studies have shown that when *IRF4* is downregulated in myeloma cells, cell death occurs, indicating the importance of *IRF4* in myeloma cell survival (Shaffer et al., 2008). The same study found that increasing *MYC* expression in myeloma cells led to an increase in *IRF4* in the cells, which indicated that *MYC* and *IRF4* regulate each other (Shaffer et al., 2008). Both *MYC* and *IRF4* are important for myeloma cell survival, making them attractive therapeutic targets.

Effective IMiD responses result in the downregulation of *MYC* and *IRF4*. When IKZF1 and IKZF3 are depleted as a result of IMiDs, a previous study saw a decrease in the amount of *IRF4* mRNA (Krönke et al., 2014). IKZF1 and IKZF3 also regulate the expression of *MYC*, which indicates that IMiDs can also downregulate *MYC* (Neri et al.,

2024; Welsh et al., 2024). Thus, IMiDs are effective because they downregulate the major transcription factors that regulate plasma cell identity and myeloma survival.

Immunomodulatory Drug Resistance

A significant problem with the management of Multiple Myeloma is that many patients develop resistance to IMiDs. It takes patients approximately 5 years to become refractory to lenalidomide (Joseph et al., 2020). There have been a few proposals for the mechanisms behind resistance. In previous studies, it has been found that mutations in Cereblon (CRBN) led to pomalidomide and lenalidomide resistance. In Gooding et al. (2021), whole genome sequencing was conducted on four hundred and fifty-four patients, and in patients with refractory/relapsed Multiple Myeloma, the progression-free survival rate was significantly shorter in patients with CRBN mutations compared to patients that did not have CRBN mutations (Gooding et al., 2021). This is a significant finding as these CRBN mutations are believed to inhibit IMiD-CRBN binding, thus preventing the efficacy of IMiDs. Other papers have corroborated CRBN mutations in IMiD-resistant patients (Jones et al., 2021), and follow-up studies have functionally confirmed that many of the CRBN mutations reported in patients induce IMiD resistance in cell line models (Chrisochoidou et al., 2025.). However, these mutations only happened in a fraction of IMiD-resistant Multiple Myeloma patients, indicating other mechanisms also cause IMiD resistance (Jones et al., 2021).

In 2024, Neri et al. and Welsh et al. found that IKZF1 and IKZF3 were consistently depleted by lenalidomide and pomalidomide across a panel of over 40 Multiple Myeloma cell lines, which included both IMiD-sensitive myeloma cells such as H929 and MM1S as well as IMiD-resistant myeloma cells such as RPMI8226 and JJN3 (Neri et al., 2024;

Welsh et al., 2024). However, only the IMiD-sensitive cells downregulated *MYC* and *IRF4*, which suggests that IMiD-resistant myeloma cells have a mechanism to maintain *MYC* and *IRF4* independently of IKZF1 and IKZF3. Further, in some IMiD-resistant cells, the ETS-family transcription factor ETV4 was found to bind the enhancers of *MYC* and *IRF4* maintaining their expression independently of IMiDs, IKZF1 and IKZF3 (Neri et al., 2024). Similarly, Welsh et al. (2024) found that the AP-1 transcription factors BATF, BATF2, and BATF3 can maintain *MYC* and *IRF4* expression and induce IMiD resistance. This is shown in **Figure 1**, where transcription factors such as BATF, BATF2, BATF3, ETV4, and potentially other transcription factors can maintain *MYC* and *IRF4* independently of IKZF1 and IKZF3. While these transcription factors are potential drug targets, there are limited candidate molecules that target them directly. Additionally, BATF and ETV4 factors are heterogeneously expressed and often only present in a subset of patients; thus, targeting such factors directly would not yield a generalizable approach for overcoming IMiD resistance (Neri et al., 2024; Welsh et al., 2024).

Targeting Transcriptional Co-Activators

A more generalizable approach to targeting heterogeneously expressed transcription factors that can induce IMiD resistance is to target the common co-activators necessary to facilitate gene expression. EP300 and CBP transcriptional co-activators catalyze acetylation on histone 3 lysine 27 (H3K27ac) (Delvecchio et al., 2013). Acetylation of histones allows DNA to be transcribed into mRNA, increasing gene expression. The bromodomains of EP300 and CBP are required for binding acetylated histones, specifically H4K12ac and H3K18ac (Delvecchio et al., 2013). EP300 and CBP play roles in the development of cancer, as they are protein interaction mediators, and they increase

and maintain gene expression by regulating enhancers of genes (Vannam et al., 2021). EP300 and CBP are also known to regulate *MYC* and *IRF4*, making them therapeutically attractive strategies for targeting *MYC* and *IRF4* (Conery et al., 2016). EP300/CBP inhibitors arrest the myeloma cells in G1 of the cell cycle, which is a phase of the cell cycle where DNA is being prepared to be replicated and the cell is growing as well as organelles (Conery et al., 2016). Arresting the cells in the G1 phase, inhibits the replication of DNA, and therefore, Multiple Myeloma cells undergo growth arrest. When the cell cycle cannot proceed past G1, they are moved to G0, where myeloma cells undergo apoptosis; therefore, cell death is expected with EP300/CBP inhibition. It was found that when myeloma cells were treated with an EP300/CBP inhibitor, *IRF4* was suppressed within two hours of being dosed, which indicates that EP300/CBP inhibition has effects on the gene regulation of multiple myeloma cells as well as the cell's viability (Conery et al., 2016).

To more effectively target myeloma biology, EP300/CBP inhibitors have been developed and are currently in phase 2 clinical trials. Inhibiting EP300/CBP decreases myeloma cell viability and suppresses gene expression of major transcription factors that keep myeloma proliferating, including *IRF4* and *MYC*. CCS1477 is an EP300/CBP inhibitor that targets the bromodomain of EP300/CBP, inhibiting the binding of EP300/CBP to H4K12ac and H3K18ac and therefore inhibits the acetylation of histone 3 lysine 27 (Nicosia et al., 2023). Nicosia et al. used CCS1477 on Multiple Myeloma cells found that CCS1477 inhibited the growth of myeloma cells by inducing cell cycle arrest (Nicosia et al., 2023). The same study found that CCS1477 led to a redistribution of EP300 and CBP genomic binding away from enhancers of *MYC* and *IRF4*, which led to

the downregulation of *MYC* and *IRF4*, leading to a disruption of proto-oncogenic activity (Nicosia et al., 2023). In a previous study, a similar EP300/CBP bromodomain inhibitor, GNE781, was used in combination with IMiDs (Welsh et al., 2024). This study showed that IMiDs effectively depleted IKZF1 and IKZF3 in both IMiD-sensitive and resistant cells. However, IMiD-resistant myeloma cell lines still maintained *MYC* and *IRF4*, suggesting that IMiD-resistant cells maintain *MYC* and *IRF4* expression using other transcription factors. The EP300/CBP inhibitor GNE781 combined with an IMiD was able to downregulate *MYC* and *IRF4* and reduce myeloma cell viability more effectively (Welsh et al., 2024). The data in this study indicate that combining IMiDs with EP300/CBP inhibition results in a more significant drop in *MYC* and *IRF4* and an increase in apoptosis of the myeloma cells (Welsh et al., 2024).

Research Aims

For years, immunomodulatory drugs have been the standard treatment for Multiple Myeloma as they deplete the transcription factors necessary for disease growth: IKZF1 and IKZF3. Still, Multiple Myeloma cells eventually become resistant, potentially due to Cereblon (CRBN) mutations, enhancer mutations, and many more possibilities. Two other major players are involved in the progression of myeloma disease, *MYC* and *IRF4*, which also play a role in acquiring IMiD resistance in myeloma cells. Currently, we are unable to target *MYC* and *IRF4* directly as they are “hard-to-treat” targets and we need to find ways to treat them to combat IMiD resistance indirectly. Some attractive therapeutic targets for this include EP300 and CBP. These therapies work by decreasing available chromatin binding sites and have been proven effective in downregulating *MYC* and *IRF4*. With the available research on using EP300/CBP inhibitors alone and in combination with

IMiDs, it is important to study the synergy between EP300 inhibitors and IMiDs, as they have the potential to add more treatment options for Multiple Myeloma patients as well as add to the conversation of how to prevent IMiD resistance.

This thesis aims to determine the therapeutic synergy between immunomodulatory drugs and EP300/CBP inhibitors by understanding how this combination downregulates oncogenic enhancers that lead to therapeutic resistance, as well as decreasing the viability of myeloma cells.

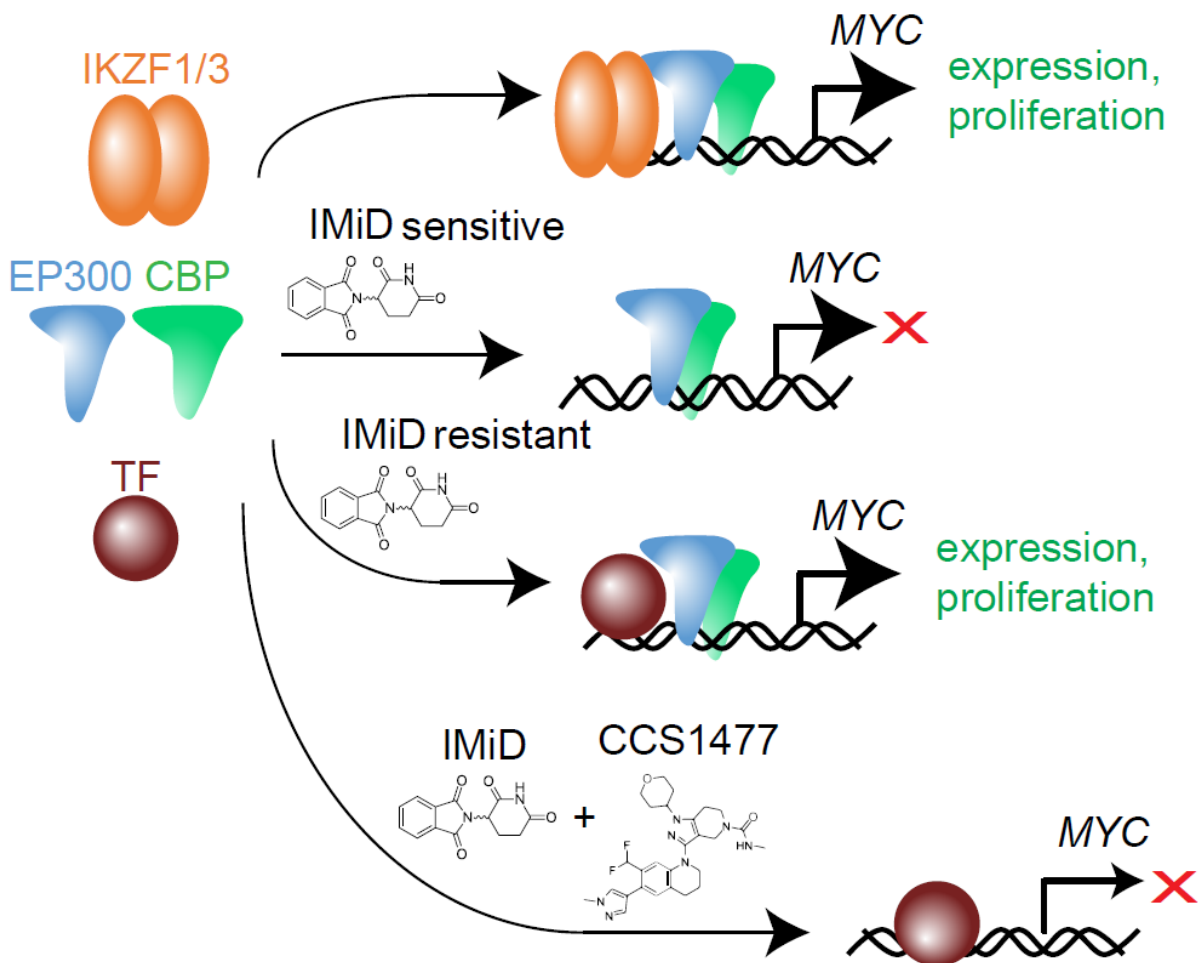


Figure 1. Model of IKZF1, IKZF3, EP300, CBP, and other transcription factors (TF) regulating MYC in Multiple Myeloma

In Multiple Myeloma cells, IKZF1, IKZF3, EP300, and CBP bind at the enhancers of *MYC* and *IRF4*, leading to *MYC* and *IRF4* expression and Multiple Myeloma proliferation (first arrow). IMiDs result in the depletion of IKZF1 and IKZF3 (second arrow). However, other transcription factors (TFs) can substitute for IKZF1 and IKZF3 to maintain *MYC* and *IRF4* expression, which leads to IMiD resistance (third arrow) (Neri et al., 2024; Welsh et al., 2024). When myeloma cells are treated with IMiDs and an EP300/CBP inhibitor (CCS1477), IKZF1 and IKZF3 are depleted, and EP300 and CBP are inhibited, resulting in downregulation of *MYC* and other oncogenes in myeloma (fourth arrow).

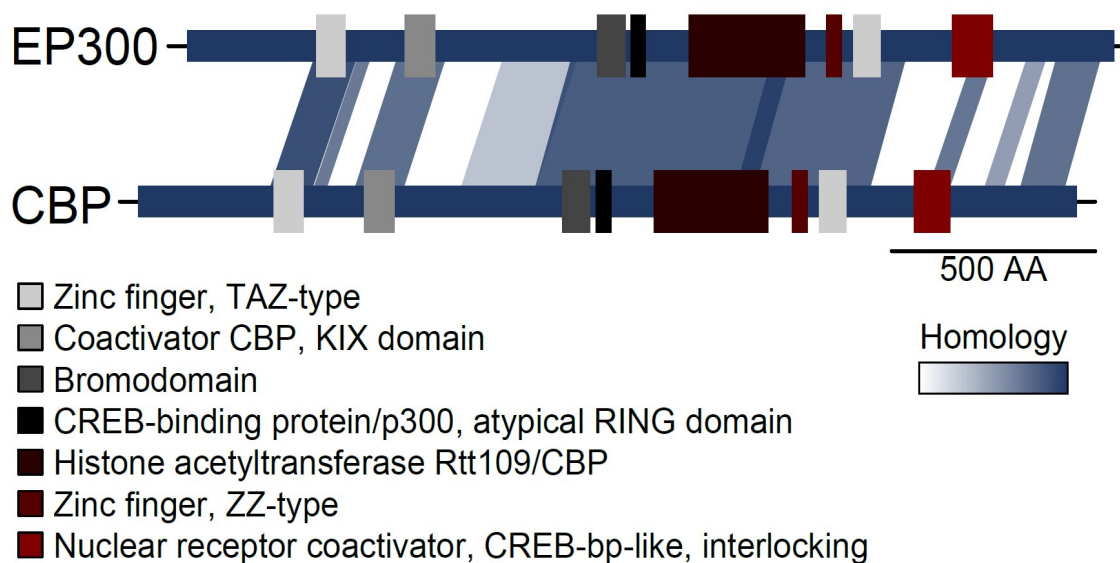


Figure 2. EP300 and CBP are paralogous histone acetyltransferases.

Protein homology between EP300 and CBP where homologous regions of EP300 and CBP are denoted by blue bars connecting the regions from each protein. Protein domains are annotated (key bottom left), including the bromodomain and the histone acetyltransferase domain.

Methods

Cell Lines

We used myeloma cell lines KMS26 (gift from the Boise Lab), RPMI8226 (ATCC), MM1S (ATCC), H929 (ATCC), and JJN3 (gift from Steinberger et al., 2019) for cell viability dose curves. We used JJN3 D11, which has a MYC-EGFP reporter for the MYC expression dose curves (gift from Steinberger et al., 2019). These cells were cultured under room temperature and sterile conditions.

Sample preparation

4,400,000 cells were collected per cell line and spun down in a 50 mL Conical Bottom Centrifuge Tube, Graduated, Sterile, made with polypropylene plastic (430828; Corning®) in the Eppendorf Centrifuge 5180 R at 300g for five minutes. The excess liquid was discarded so that only the pellet was left, and the cells were resuspended in 22 mL of media made of 87% RPMI1640 (Corning), 1% PenStrep (Corning), 1% L-Glutamine (Corning), 1% HEPES Buffer (Corning), and 10% FBS. The cells were then plated in a 96-well flat-bottom plate with 200 μ L volume per well at a concentration of 200,000 cells / mL. After the cells were treated with either pomalidomide (19171-19-8; MedChemExpress), CCS1477 (gift from CellCentric), or both as described below. The cells were assessed with flow cytometry 48 and/or 96 hours after treatment.

Serial Dilution of CCS1477

A stock concentration of CCS1477 at 10 mM was diluted to 16 μ M by doing a 1:100 dilution followed by a 16:100 dilution using Phosphate Buffered Saline (PBS) as the dilutant in a 1.5 mL Seal-Rite sterile tube (1615-5510; USA Scientific). 10 μ L of the 16 μ M solution was added to 200 μ L of cell culture for a final concentration of 800 nM. Serial

dilutions of 400 nM, 200 nM, 100 nM, 50 nM, 25 nM, and 12.5 nM were created using a 1:2 dilution ratio. Similarly, 10 μ L of these solutions were added to 200 μ L of cell culture in 96-well flat bottom plates (29442-054; Corning®) using a p20 Rainin multichannel.

Serial Dilution of pomalidomide

A stock of pomalidomide with a concentration of 25 mM was diluted to 8 μ M by doing a 1:100 dilution followed by a 32:1,000 dilution using PBS as the dilutant in a 1.5 mL Eppendorf tube. 10 μ L of the solution was added to 200 μ L of cell culture for a final concentration of 400 nM. Serial dilutions of 200, 100, 50, and 25 nM were created using a 1:2 dilution ratio. Similarly, 10 μ L of these solutions were added to 200 μ L of cell culture in a 96-well flat bottom plate using a p20 Rainin Multichannel.

Annexin V and Live/Dead Staining and Data Collection

FITC-labelled counting beads (335925; BD) were used to count cells by flow cytometry on a BD (Becton Dickinson) FACSymphony A1. Flow cytometry measures cells in a single-cell stream collected by the flow cytometer. When samples were loaded into the flow cytometer, lasers within the flow cytometer were used to excite fluorophores or fluorescent proteins, such as EGFP, and the emission spectrum is collected using a series of detectors. Additionally, the cells' forward and side scatter properties are measured, representing the cell volume, textures, and irregularities, which gives us estimates of the viability of the cells (Hawley & Hawley, 2010). In addition to the forward and side scatter lasers, some detect fluorescence in cells. This has great therapeutic implications for Multiple Myeloma patients who have undergone several different treatments and have become resistant to IMiDs. For example, the JLN3 D11 cells used

were engineered to have an *MYC*-EGFP reporter (Steinberger et al., 2019). Flow cytometry can be used to excite EGFP (using the 488 nm laser) and capture the EGFP fluorescence using the 530 nm detector as a proxy of *MYC* gene expression in the cells.

Following the Annexin protocol, we made a master mix of 0.04 μL of GhostDye Red780 (Cyttek #13-0865-T100), 0.4 μL of Annexin V (Cytotek #35-6409-T100) per 100 μL of Annexin Buffer (0.1 M HEPES, 1.4 M NaCl, and 25 mM CaCl_2 solution (Sigma #C-5080), filtered H_2O , and 0.22 μM filter Fisher (09-719A)). The cells were then transferred from a 96-well flat-bottom plate to a 96-well round-bottom plate and spun in the centrifuge at 300g for five minutes. The excess liquid was discarded, and the pellets were resuspended with 100 μL of Annexin master mix and then incubated for fifteen minutes at room temperature. The cells were resuspended in 200 μL of Annexin buffer and transferred to 1.2 mL tubes.

Annexin V binds to phosphatidylserine, which is typically found on the inner cell membrane. During apoptosis, phosphatidylserine is flipped to the outer membrane, allowing Annexin V to bind cells that are undergoing apoptosis (Miller, 2004). Using the flow cytometer, Annexin V-FITC can be detected using the blue laser (488 nm) and capturing FITC emission at 530 nm. Ghost Dye Red780 is a live/dead (L/D) dye that detects the percentage of dead cells. These types of L/D dyes are non-cell permeable and bind to free amines. Thus, only when a cell membrane is compromised will live/dead dyes react with the free amines within a cell. Therefore, staining with both Annexin V-FITC and Ghost Dye Red780 allows for the simultaneous detection of cells that are early in apoptosis (Annexin V+ L/D-) and those later in the apoptotic process (Annexin V+ L/D+).

Annexin V-FITC and live/dead staining were measured on the BD FACSymphony A1 using the red laser (633 nm) and the 780/60 detector and the blue laser (488 nm) with the 530/30 detector, which detect the Annexin V dye and Ghost Dye 780, respectively. Ten thousand events were collected and analyzed through the flow cytometer per sample.

Data Analysis

The flow cytometer data was analyzed using FlowJo (Becton Dickinson) to count the number of cells alive, Annexin-positive cells (undergoing apoptosis), and dead cells. FlowJo was then used to make contour plots based on the cell counts, and R Studio was used to develop viability curves based on varying doses of pomalidomide and CCS1477.

The FlowJo counts were also placed into a synergy finder (synergyfinder.fimm.fi) to determine if there is synergy between pomalidomide and CCS1477. The synergy finder uses a Zero Interaction Potency (ZIP) model to calculate a score to determine the amount of synergy between pomalidomide and CCS1477. This model compares the observed combination response to the expected effect of the two drugs separately. The drug combination is deemed synergistic when the observed combination response is greater than the expected effect (Yadav et al., 2015). When the observed combination response is less than expected, the drug combination is deemed not synergistic or antagonistic (Yadav et al., 2015).

Results

IMiD and EP300/CBP Inhibitor Modulation of *MYC* Expression as Measured in JJN3 D11

To examine whether a combination of CCS1477 and pomalidomide can downregulate *MYC* expression, we used a myeloma cell line that expresses Enhanced Green Fluorescent Protein (EGFP) co-translationally with the *MYC* oncogene. Specifically, the *MYC* locus of JJN3 cells was genetically edited with CRISPR/Cas9 to insert a protein cleavage domain (P2A) and a version of EGFP with a PEST domain (d2EGFP) that confers a short half-life to EGFP (~2 hrs as compared to 26 hrs normally) (Steinberger et al., 2019). Thus, in these cells (hereafter referred to as JJN3 D11), as *MYC* is transcribed and translated, d2EGFP is also generated, which can be measured as a proxy of *MYC* expression. Since the d2EGFP has a short half-life, conditions that inhibit *MYC* expression will decrease EGFP expression in a matter of hours.

Treating JJN3 D11, the *MYC*-d2EGFP reporters, with both pomalidomide and CCS1477, we see that on Day 2, the *MYC* expression as measured by EGFP was lower (orange curve) than either 200 nM of pomalidomide (blue) and 200 nM of CCS1477 (black) alone (**Figure 3A**). The combination curve closely matches the parental cell line, as noted by the light grey peak, which contains no EGFP. By Day 4, the combination curve is almost identical to the parental curve, noting a decrease in EGFP and *MYC* expression compared to control (grey) (**Figure 3A**). CCS1477 alone leads to a 70% decrease in EGFP, but the combination does this to a greater extent (greater than 80%). **Figure 3B** depicts the EGFP by varying concentrations of pomalidomide and CCS1477, on day two, there is a 40% decrease in EGFP when the cells are treated with just pomalidomide (0 nM on x-axis) and CCS1477 alone (grey line). Still, the greatest decrease is seen when pomalidomide and CCS1477 are in combination (black, green, and blue lines). Day four illustrates similar results as day two; however, IMiD resistance is more apparent in these

cells on day four, as even at the highest dose of pomalidomide (200 nM), there is no change in EGFP. When CCS1477 is added, there is a great decrease in EGFP, especially in combination (**Figure 3B**).

We estimated viability using the cells' forward scatter and side scatter characteristics measured by flow cytometry (**Figure 3B**). Dead cells with compromised membranes are often smaller in size (measured by forward scatter) and more granular (measured by side scatter). Using this approach, we estimated increased cell death in the combination-treated cells on day four compared to day two where there was no change in cell death (**Figure 3B**).

IMiD-Resistant Cell Lines

The above data suggested that the combination of CCS1477 and pomalidomide induced cell death in JJN3, an IMiD-resistant cell line. To more directly measure cell death, we used parental JJN3 cells, JJN3 cells without the *MYC*-EGFP reporter, and repeated the dose curve experiments followed by staining with Annexin V and Live/Dead Dye (L/D). When JJN3 is treated with 400 nM of pomalidomide and 0 nM of CCS1477 (**Figure 4A**, bottom left), 6.6% of cells are Annexin V+ and 10.7% of cells are L/D+, illustrating JJN3's IMiD-resistance. JJN3 is sensitive to CCS1477 as when JJN3 is treated with 800 nM of CCS1477 and 0 nM of pomalidomide (**Figure 4A**, top right) there are 13.4% of cells that are Annexin V+ and 46.9% of cells that are L/D+. However, the combination of pomalidomide and CCS1477 in combination (**Figure 4A**, bottom right), there is the greatest amount of apoptosis and cell death with 26.3% of cells that are Annexin V+ and 51.6% of cells that are L/D+. **Figure 4B** illustrates the effect of pomalidomide and CCS1477 in varying doses on JJN3. At 0 nM of CCS1477, IMiD-resistance is prominent

as there is not a big change in viability when the cells are treated in increasing doses of pomalidomide. However, we can see that the combination of pomalidomide and CCS1477 induces greater amounts of cell death, especially in the higher doses of drugs as the viability drops to 30% viable. We can also see that the combination doses are closest in viability to each other at 400 nM of pomalidomide and 800 nM of CCS1477. When analyzing the synergy of pomalidomide and CCS1477 in JJN3, we can see in **Figure 4C** that this drug combination had a Zero Interaction Potency (ZIP) score for the combination in JJN3 was 0.8, indicating that there is synergy in certain combination doses. Looking at the heat map, the combination is synergistic with high doses of CCS1477 combined with pomalidomide as the brighter the red, the greater the synergy. The greatest synergy is with doses of CCS1477 greater than 200 nM and doses of pomalidomide greater than 100 nM.

RPMI8226 is also an IMiD-resistant cell line. This is evident from the CCS1477 and pomalidomide dose curves, which show almost no increase in cell death even at the highest dose of pomalidomide (**Figure 5A**). Looking at **Figure 5A**, we can visualize the percentage of cells that are Annexin V + and L/D +, there is small percentage of cells that are Annexin V + and L/D + (7.6% and 8.8%). Below the control we see the treatment of 0 nM of CCS1477 and 400 nM of pomalidomide. Here, we can see that even with 400 nM of pomalidomide, cell death, and apoptosis are almost equivalent to the control. Cells treated with the highest dose of CCS1477 (800 nM) and 0 nM of pomalidomide had about 51% of cells that are Annexin V+, and roughly 16% L/D+ cells. At a combination of 800 nM of CCS1477 and 400 nM of pomalidomide, there is a higher percentage of dead cells, with roughly 29% L/D+ and 53% Annexin V+. This Annexin V plot indicates that we see

the greatest amount of myeloma cell death when pomalidomide and CCS1477 were in combination and that this combination works in IMiD-resistant cell lines. Data from three experiments are summarized in **Figure 5B**, which shows that the addition of CCS1477 reduces the viability of these IMiD-resistant cells starting at 100 nM of CCS1477. The synergy between pomalidomide and CCS1477 is low, with the synergy ZIP score being -4.368, and it is only synergistic at very high doses of pomalidomide (above 100 nM) and CCS1477 (above 200 nM) (**Figure 5C**).

IMiD-Sensitive Cell Lines

H929 is an IMiD-sensitive cell line. **Figure 6A** depicts the percentage of cells that are Annexin V+ (apoptotic) and Live/Dead (L/D) + (dead). When H929 is dosed with 400 nM of pomalidomide and no CCS1477 (**Figure 6A**, bottom left), 31.3% of the cells are Ghost Dye positive, otherwise dead, and 18.5% of H929 are Annexin V positive, i.e., undergoing apoptosis. H929 was also sensitive to EP300/CBP inhibition as 800 nM of CCS1477 (top right plot), and no pomalidomide resulted in 60.3% of the cells being L/D+ and 20.7% undergoing apoptosis. However, when pomalidomide and CCS1477 are in combination at the highest dose of both drugs (bottom right plot), we can see the largest drop in viability where 80.2% of the cells are L/D+ and 16.8% are Annexin V+. **Figure 6B** illustrates the effect of the combination of pomalidomide and CCS1477 at varying doses of both drugs. At 0 nM CCS1477, we can see that pomalidomide does affect H929 viability, which supports the IMiD sensitivity of H929. However, there is a remarkable decrease in viability when CCS1477 is added in increasing doses, and we can see that viability drops to below 20% as the doses increase. We can also see that after 200 nM of pomalidomide and 200 nM of CCS1477, the effect of the drugs on H929 viability is similar.

When analyzing the synergy of pomalidomide and CCS1477 in H929, we can see in **Figure 6C** that this drug combination is very synergistic. This synergy was most apparent between 200 nM and 400 nM of CCS1477 and between 50 nM and 200 nM of pomalidomide as the heat map in **Figure 6C** indicates the brightest shade of red, indicating the highest level of synergy.

MM1S is an IMiD-sensitive cell line. Looking at **Figure 7A**, at the highest dose of pomalidomide (bottom left plot), there is 26.9% cells that are L/D+ and 17.2% cells that are Annexin V+. When 800 nM of CCS1477 is added, cell death increases to 50.7%, and 34.9% of cells undergoing apoptosis. **Figure 7B** depicts the effect of pomalidomide and CCS1477 on MM1S viability at increasing doses of both drugs. Between 0 nM of pomalidomide and 400 nM of pomalidomide, the viability decreases from approximately 90% to below 70%. CCS1477 induces a more significant decrease in viability; at 800 nM, the viability reaches approximately 40%. However, the largest decrease in viability is when pomalidomide and CCS1477 are in combination, where after 200 nM of CCS1477 and 25 nM of pomalidomide, the viability reaches 20%. **Figure 7C** depicts the synergy between CCS1477 and pomalidomide in MM1S, and based on the synergy ZIP score of 8.52, the two drugs are very synergistic in the MM1S myeloma cell line, especially after 50 nM of CCS1477 and above 100 nM of pomalidomide has the brightest red, indicating the most synergistic combinations of CCS1477 and pomalidomide.

KMS26 is an IMiD-sensitive cell line and, when there is no CCS1477, the viability of KMS26 decreases as pomalidomide increases (**Figure 8A**). The response to CCS1477 decreases as the dose of CCS1477 increases and when treated in combination with pomalidomide, but the response was not as drastic as RPMI8226. Looking at the Annexin

and Live/Dead data, with 400 nM of pomalidomide and no CCS1477 (**Figure 8A**, bottom left), 16.59% of the cells are L/D + and 27.3% are Annexin V+ L/D-, indicating they are actively undergoing apoptosis. The 800 nM dose of CCS1477 indicates that 21% of the cells are L/D+, and 15.4% are Annexin V+ L/D-. There is an increase in the number of cells that are dead and undergoing apoptosis in the combination trial, where we see 24.6% of cells are L/D+ (**Figure 8A**, bottom right sample, top right quadrant), and 34.7% of cells are Annexin V+ live/dead-, suggesting they are undergoing apoptosis (**Figure 8A**, bottom right sample, bottom right quadrant). **Figure 8B** depicts the viability change by doses of pomalidomide and CCS1477. There is a decrease in viability by increasing doses of pomalidomide and CCS1477. However, KMS26 differs from the other tested IMiD-sensitive cell lines, H929 and MM1S, as it was less sensitive to CCS1477. With no pomalidomide, 800 nM of CCS1477 does not decrease as much as the other IMiD-sensitive cell lines. While the combination of pomalidomide and CCS1477 does decrease the cell viability to a greater extent than the drugs alone, the change in viability is less than the other IMiD-sensitive cell lines above. **Figure 8C** depicts the synergy of pomalidomide and CCS1477 in KMS26, which does not have a lot of synergy, with the ZIP score being -6.134.

Results Summary

Our results indicate that there was a greater decrease in *MYC* expression when pomalidomide and CCS1477 were used in combination than alone. All cell lines displayed greater decreases in viability when pomalidomide and CCS1477 were in combination. The IMiD-sensitive cell lines, H929 and MM1S, saw the greatest amount of synergy as noted by the ZIP score, and the IMiD-resistant cell lines were synergistic at higher

doses of pomalidomide and CCS1477 (200 nM and above). KMS26 did not show much synergy according to the ZIP score.

Figure 3

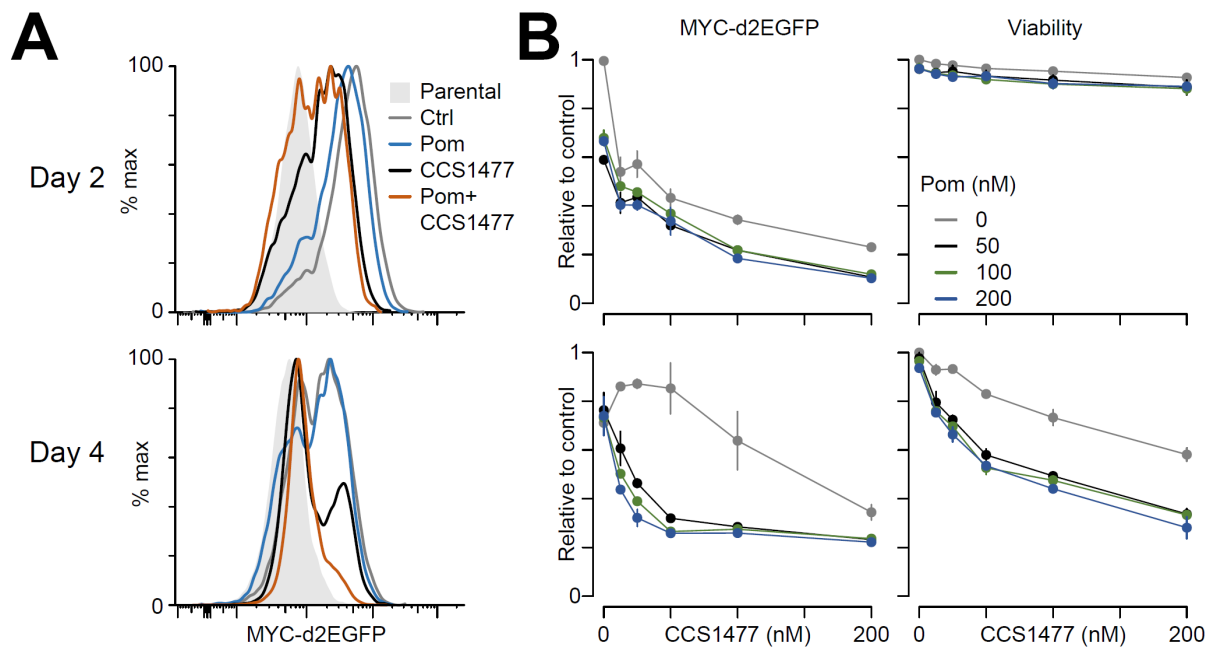


Figure 3A-B. IMiD and EP300/CBP Inhibitor Modulation of *MYC* Expression as Measured in JJN3 D11

A. JJN3 D11 *MYC*-d2EGFP expression in response to 200 nM pomalidomide, 200 nM CCS1477, or the combination of both on days 2 and 4. **B.** Viability of JJN3 D11 is estimated by the forward scatter and side scatter characteristics on flow cytometry and shown in response to varying doses of pomalidomide and CCS1477.

Figure 4

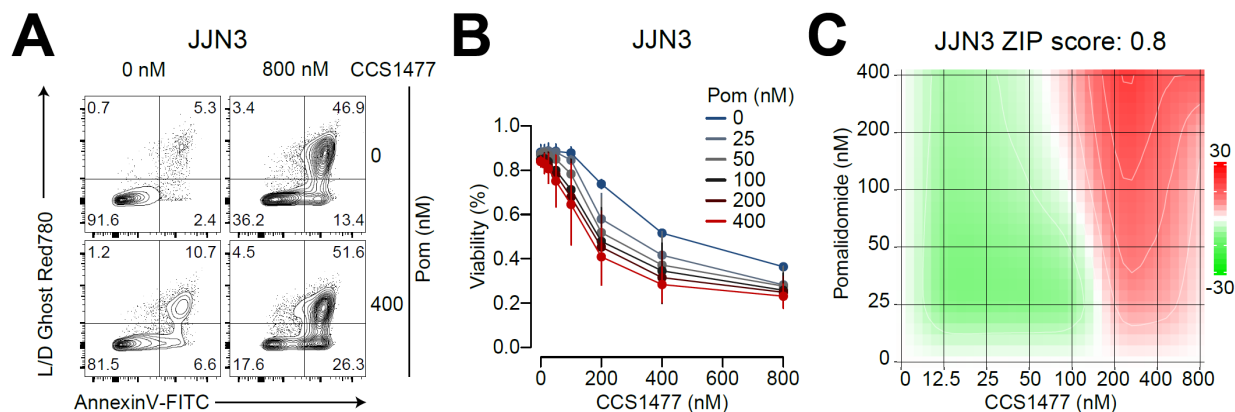


FIGURE 4A-C. Viability and Synergy Plots for JJN3

A, Flow cytometry of JJN3 myeloma cells stained with Annexin V and Live/Dead (Ghost Dye Red780) untreated (top) or treated with 400 nM pomalidomide (Pom; bottom), and/or 800 nM CCS1477 (right). **B**, Summarized viability (Live/Dead-, Annexin V-) in response to pomalidomide and CCS1477 (x-axis). **C**, Heat map of H929 dosed with pomalidomide and CCS1477 depicting synergy between the drugs at varying dose combinations.

Figure 5

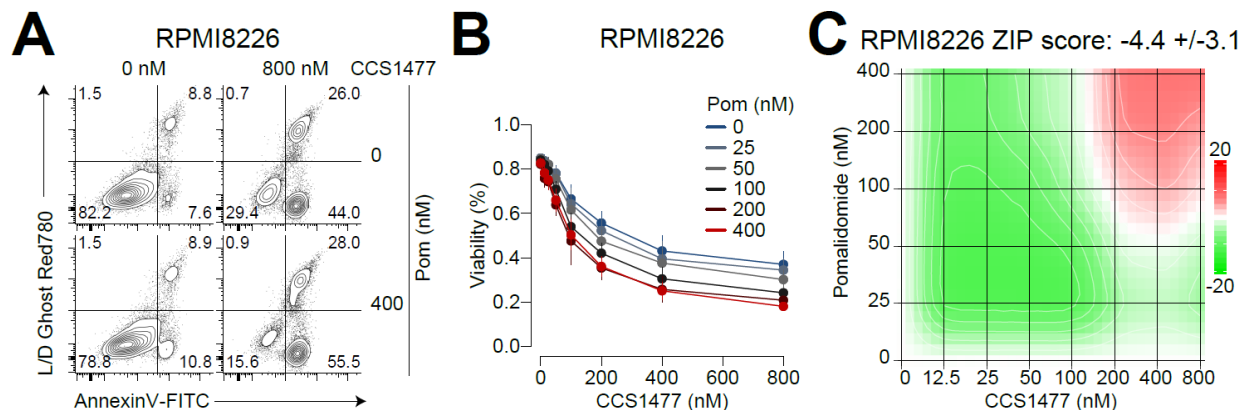
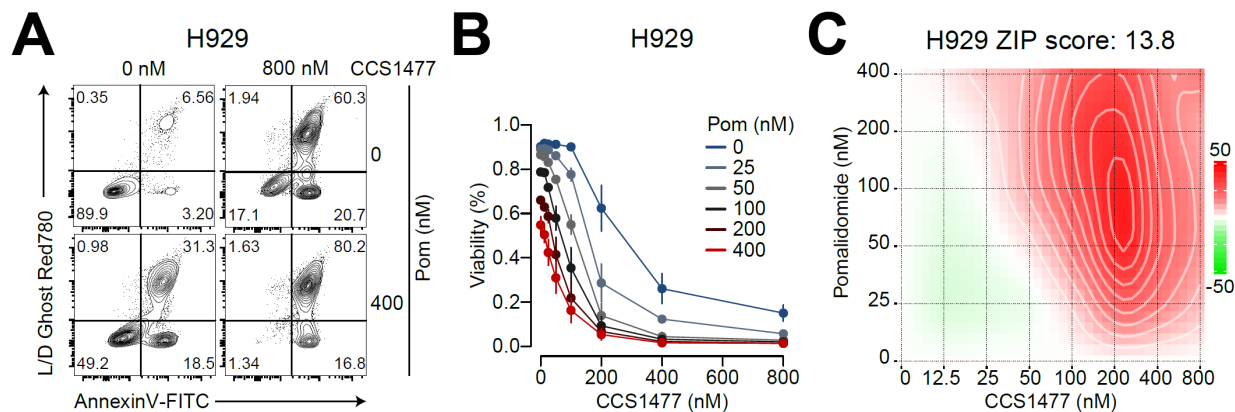


FIGURE 5A-C. Viability and Synergy Plots for RPMI8226

A, RPMI8226 viability (Live/Dead-, Annexin V-) in response to pomalidomide and CCS1477 (x-axis). Mean and SE are shown (N=3). **B**, Flow cytometry of Annexin V and Live/Dead (Ghost Dye 780) with pomalidomide (Pom) untreated (top) and 400 nM (bottom) and with CCS1477 untreated (left) and 800 nM (right). **C**, Heat map of RPMI8226 dosed with pomalidomide and CCS1477 depicting synergy between the drugs at varying dose combinations.

Figure 6**FIGURE 6A-C. Viability and Synergy Plots for H929**

A, Flow cytometry of H929 myeloma cells stained with Annexin V and Live/Dead (Ghost Dye Red780) untreated (top) or treated with 400 nM pomalidomide (Pom; bottom), and/or 800 nM CCS1477 (right). **B**, Summarized viability (Live/Dead-, Annexin V-) in response to pomalidomide and CCS1477 (x-axis). **C**, Heat map of H929 dosed with pomalidomide and CCS1477 depicting synergy between the drugs at varying dose combinations.

Figure 7

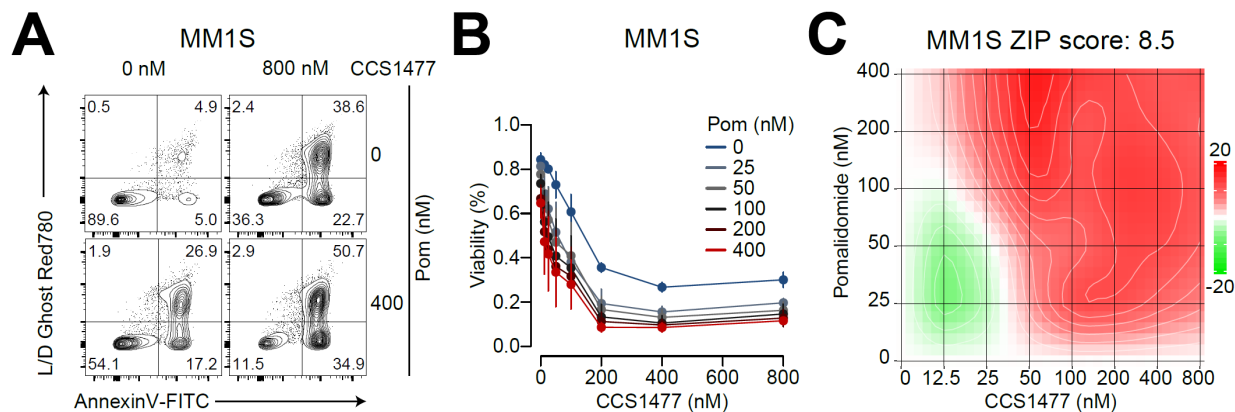
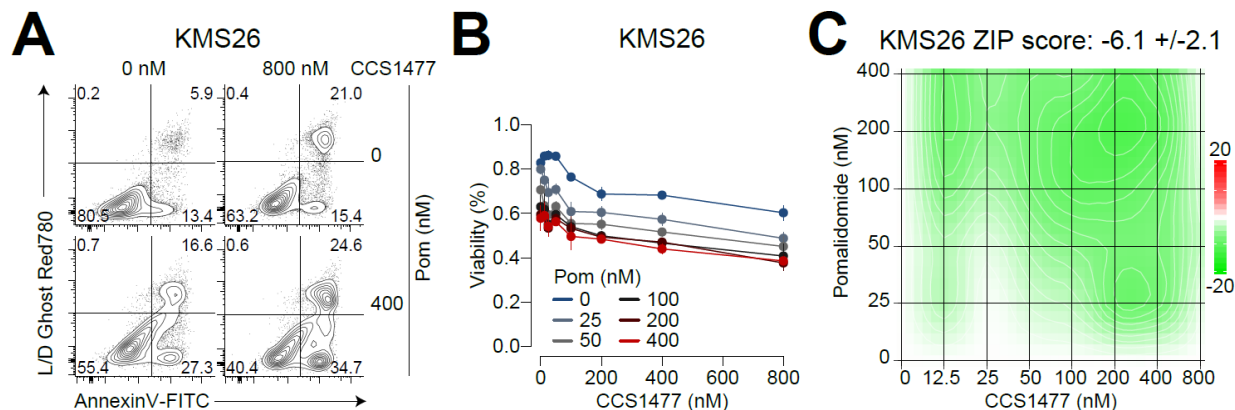


FIGURE 7A-C. Viability and Synergy Plots for MM1S

A, Flow cytometry of MM1S myeloma cells stained with Annexin V and Live/Dead (Ghost Dye Red780) untreated (top) or treated with 400 nM pomalidomide (Pom; bottom), and/or 800 nM CCS1477 (right). **B**, Summarized viability (Live/Dead-, Annexin V-) in response to pomalidomide and CCS1477 (x-axis). **C**, Heat map of H929 dosed with pomalidomide and CCS1477 depicting synergy between the drugs at varying dose combinations.

Figure 8**FIGURE 8A-C. Viability and Synergy Plots for KMS26**

A, Flow cytometry of KMS26 myeloma cells stained with Annexin V and Live/Dead (Ghost Dye Red780) untreated (top) or treated with 400 nM pomalidomide (Pom; bottom), and/or 800 nM CCS1477 (right). **B**, Summarized viability (Live/Dead-, Annexin V-) in response to pomalidomide and CCS1477 (x-axis). **C**, Heat map of KMS26 dosed with pomalidomide and CCS1477 depicting synergy between the drugs at varying dose combinations.

Discussion

Overview

The development of IMiD resistance is a challenge in treating Multiple Myeloma. Previous studies have proposed that mechanisms of resistance are caused by mutations in Cereblon that abrogate its ability to bind IMiDs, resulting in reduced ubiquitination and proteasomal degradation of Ikaros (IKZF1) and Aiolos (IKZF3). However, these mutations have only been found in a small percentage of myeloma patients (Gooding et al., 2021). Other studies have found that other transcription factors such as ETV4, BATF, BATF2, and BATF3 can partially replace IKZF1 and IKZF3 function when they are degraded through the use of IMiDs (Welsh et al., 2024; Neri et al., 2024). These other transcription factors can maintain the expression of proto-oncogenes involved in the proliferation of myeloma, such as *MYC*, despite IMiD treatment. Recently, there have been several studies investigating EP300/CBP inhibitors, which represent a novel strategy for overcoming IMiD resistance. EP300 and CBP are referred to as co-activators because their histone acetyltransferase activity is needed for transcription. Thus, EP300/CBP inhibition is an especially attractive strategy for those forms of IMiD resistance that are mediated by alternate transcription factors, such as ETV4 and BATF factors. One of EP300/CBP inhibitors being used in Phase II clinical trials, CCS1477, has been seen to downregulate *MYC* and *IRF4* by binding the bromodomain of EP300 and CBP displacing them from the enhancers and promoters of *MYC* and *IRF4*. We aimed to determine if there is therapeutic synergy between EP300/CBP inhibitors and immunomodulatory drugs in various Multiple Myeloma cell lines. We conducted experiments using pomalidomide, an IMiD commonly used in second-line and later therapies (currently being

tested with CCS1477 in clinical trials), and CCS1477. These studies were conducted with IMiD-sensitive cell lines – MM1S, KMS26, H929 – and IMiD-resistant cell lines – JLN3 and RPMI8226. It was important to test this drug combination in both IMiD-sensitive and resistant cells because previous studies found that IMiD-resistant cell lines did not downregulate important proto-oncogenes in Multiple Myeloma such as *MYC* and *IRF4*, indicating that other mechanisms maintained the expression of *MYC* and *IRF4*. Our experiments tested the drug combination on both cell lines to determine if there was therapeutic synergy in IMiD-resistant and sensitive cell lines.

Results Interpretation

When we added CCS1477 and pomalidomide in combination in JLN3 D11 cells containing a *MYC*-EGFP reporter, *MYC* expression decreased to match that of the parental cells that contained no EGFP, suggesting *MYC* expression was almost completely ablated. We also noticed that on day two, *MYC* expression was decreased with pomalidomide alone; however, by day four, *MYC* expression rebounded and showed resistance to pomalidomide. With the addition of CCS1477, there was a great reduction in *MYC* expression, even at the lower doses (50 nM) of pomalidomide. This indicates that the combination of CCS1477 and pomalidomide was able to overcome IMiD resistance in a myeloma cell line. We also looked at the effects of the drug combination on the viability of the Multiple Myeloma cell lines. We found that in all cell lines, including the IMiD-resistant cell lines, the combination of CCS1477 and pomalidomide decreased the viability of the cells to a greater extent than just pomalidomide and/or just CCS1477. We also found that the drug combination increased the number of Annexin V+ cells, indicating this combination induces apoptosis. When we calculated the synergy between CCS1477

and pomalidomide in the synergy finder, we found that there was a significant synergy in MM1S (8.52 +/-5.73) and H929 (13.8 +/-3.23), which are both IMiD-sensitive cell lines. However, while KMS26 is also an IMiD-sensitive cell line, there was not much synergy found, with the synergy score being -6.134 +/- 2.13, which is very different from the other two IMiD-sensitive cell lines. The IMiD-resistant cell lines, RPMI8226, saw synergy only at the highest doses of pomalidomide and CCS1477, whereas JLN3 was synergistic when doses of 200 nM and more of CCS1477 were in combination with any dose of pomalidomide.

A previous study that used an EP300/CBP bromodomain inhibitor that is similar to CCS1477, GNE781, saw similar results where there was synergy in JLN3 at higher doses of CCS1477 with almost all doses of pomalidomide (Welsh et al., 2024). They also measured Annexin V and Live/Dead stain to determine viability. They also used a combination of 200 nM of pomalidomide and 40 nM of GNE781 and found that after 72 hours, the combination had the greatest amount of cells that were Annexin V+ and Live/Dead+, meaning that there was more apoptosis and cell death with the combination of pomalidomide and an EP300/CBP inhibitor (Welsh et al., 2024). MYC protein was also measured with the combination, and they found that the combination decreased the amount of MYC protein formed, which indicates that *MYC* is not being transcribed and expressed, which is similar to what we saw in the *MYC*-EGFP curves using CCS1477 (**Figure 3**; Welsh et al., 2024). Our results broadly agreed with previous publications and suggested that CCS1477 and pomalidomide are therapeutically synergistic and have the potential to downregulate *MYC* to a greater extent than either drug separately.

Comparing the viability of the cell lines, we saw the greatest decreases with the drug combination in H929 and MM1S, where at the highest dose, there was a 90% decrease in viability (**Figures 7B and 9B**). RPMI8226 and JJN3 also had a large amount of cell death with the drug combination, but at the highest dose, there was an 80% viability decrease (**Figures 3A and 8B**). KMS26 was less affected by the combination compared to the other cell lines, where the viability only decreased by about 40% (**Figure 4A**). This is an interesting case as KMS26 was sensitive to pomalidomide but not CCS1477. Future studies could explore the repertoire of transcription factors and chromatin regulators expressed in KMS26 to gain insight into why this model is resistant to EP300/CBP inhibition.

Therapeutic Implications

The combination of CCS1477 and pomalidomide has therapeutic potential in Relapsed and Refractory Multiple Myeloma patients, especially those who are IMiD resistant. In Searle et al. (2023), CCS1477 was given to a group of Relapsed and Refractory Multiple Myeloma patients, and they found that the drug combination was safe for the patients and there were mild to moderate treatment-emergent adverse effects. They also found that the drug combination, which consisted of 4 days on CCS1477 and 3 days off with 21 days of pomalidomide and dexamethasone weekly in a 28-day cycle, has promising efficacy in patients that have Relapsed and Refractory Multiple Myeloma who have been heavily pre-treated with a variety of Myeloma treatments including IMiDs (Searle et al., 2023). With CCS1477 moving on to phase 2 clinical trials, the combination of CCS1477 and pomalidomide will be tested as a therapeutic method of treatment for Relapsed and Refractory Multiple Myeloma patients. It is expected that CCS1477 will

displace EP300 and CBP from binding sites at the *MYC* and *IRF4* enhancers and promoters, which will lead to the downregulation of *MYC* and *IRF4*. Similar observations have been found in previous studies and were seen in **Figure 3A** when CCS1477 downregulated *MYC* and even more so when combined with pomalidomide (Welsh et al., 2024).

Overall, these results indicate that CCS1477 and pomalidomide are therapeutically synergistic and can downregulate *MYC* better than when used separately. This may be because CCS1477 works to move EP300 and CBP away from their cognate binding sites so that their function as coactivators is lost and, therefore, the *MYC* gene is no longer activated. Presumably, EP300 and CBP are not displaced from the *MYC* promoter and enhancer when only an IMiD is used in IMiD-resistant myeloma cases. In some IMiD-resistant cases, this results from other transcription factors beyond IKZF1 and IKZF3 that can activate *MYC*, such as BATF1, BATF2, BATF3, and ETV4 (**Figure 1**; Welsh et al., 2024; Neri et al., 2024). It has also been seen that EP300/CBP inhibitors also affect *IRF4* expression and lead to its downregulation, which can also result in Multiple Myeloma cell death as *IRF4* also plays a large role in Myeloma survival (Welsh et al., 2024).

Limitations

There were some limitations to our study. Immunomodulatory drugs are often cytostatic, inhibiting cell growth rather than killing cells. Our results only measure cytotoxicity and cell death using Live/Dead dye and Annexin V, so the full impact of pomalidomide and pomalidomide in combination with EP300/CBP inhibitors on myeloma cells remains to be elucidated. On the same note, we did not measure cell growth, but we infer that fewer cells existed in IMiD and CCS1477 combination treated conditions as the

rate of events measured on the flow cytometer at the higher doses of CCS1477 was significantly less, suggesting there was less cell growth in these conditions. Thus, the data presented here may be an underestimate of the true impact that pomalidomide and CCS1477 have on these myeloma cells.

Future Directions

There are some next steps in learning more about the role of EP300/CBP inhibitors in overcoming IMiD resistance in Multiple Myeloma. We looked at *MYC* specifically, but *IRF4* is a myeloma-specific target that both regulates *MYC* and is regulated by *MYC*. It would be interesting to see the effect of the combination of CCS1477 and pomalidomide on *IRF4* expression. This could be achieved using recently generated *IRF4*-GFP reporters to gain a larger picture of CCS1477 and pomalidomide synergy on gene expression (Bolomsky et al., 2024). It would also be valuable to test both *IRF4* and *MYC* in various cell lines, as we only tested *MYC* in an IMiD-resistant cell line, JJN3. We expect that *MYC* and *IRF4* will be downregulated in both IMiD-resistant and IMiD-sensitive cell lines. It would also be important to identify gene expression changes in IMiD-sensitive and resistant cells to identify the transcriptional responses that vary between the two and gain better insight into how to target IMiD-resistant myeloma. This could be accomplished using technologies such as RNA sequencing.

In our results and methods, we target EP300/CBP together. Still, analyzing EP300 and CBP separately may also be interesting in understanding if one plays a more prominent role in myeloma. Similarly, it would be valuable to know if inhibition of only EP300 or only CBP underlies the synergy observed with IMiDs. This could be done in future experiments using genetic approaches to knockout EP300 and/or CBP with and

without an IMiD to test their synergy profiles and whether EP300 or CBP inhibition is more or less synergistic with pomalidomide.

Previous studies have also found that EP300/CBP not only acetylates histones but also acetylates proteins such as p53 and *MYC* (Lasko et al., 2017). We could gain further insight into this mechanism through other EP300/CBP inhibitors that target the histone acetyltransferase domain, inhibiting EP300/CBP directly and its ability to acetylate histones and proteins. An EP300/CBP inhibitor that does this is A-485, which previous studies have explored (Lasko et al., 2017). This inhibitor differs from CCS1477 as it is a catalytic rather than a bromodomain inhibitor. CCS1477 binds to the bromodomain of EP300/CBP, which recognizes acetylated histones, H4K12ac and H3K18ac, and leads to the acetylation of H3K27ac. When the bromodomain of EP300 or CBP is inhibited, this blocks binding to histones and subsequent acetylation of H3K27ac. This mechanism is a less direct way of inhibiting the acetylation of histones by EP300/CBP compared to A-485. Previous studies have found that A-485 inhibited prostate cancer tumor growth (Lasko et al., 2017). It could be interesting to use this compound on myeloma cell lines and compare it to both bromodomain inhibitors such as CCS1477 and the effect on synergy with IMiDs. EP300 and CBP can also be explored further to understand whether non-histone-related functions could contribute to the therapeutic synergy observed between CCS1477 and IMiDs.

Conclusion

Our results suggest that pomalidomide and CCS1477 synergize in the IMiD-sensitive cell lines MM1S and H929 and at higher doses of CCS1477 in the IMiD-resistant cell lines RPMI8226 and JJN3. The drug combination also downregulates key target genes in

Multiple Myeloma, such as *MYC*, by moving the coactivators EP300/CBP away from the enhancer binding site, leading to the downregulation of these genes. There is still more to understand about the synergy of IMiDs and EP300/CBP inhibitors, specifically in how they affect other genes such as *IRF4* and how different EP300/CBP inhibitors can have different effects on synergy, the combination of IMiDs and EP300/CBP inhibitors has promising therapeutic use for Multiple Myeloma patients, specifically those who are Relapsed and Refractory and have gained resistance to IMiDs.

References

- Barwick, B. G., Gupta, V. A., Vertino, P. M., & Boise, L. H. (2019). Cell of origin and genetic alterations in the pathogenesis of multiple myeloma. In *Frontiers in Immunology* (Vol. 10, Issue MAY). Frontiers Media S.A. <https://doi.org/10.3389/fimmu.2019.01121121>
- Chrisochoidou, Y., Scarpino, A., Morales, S., Martin, S., Li, Y., Walker, B., Caldwell, J., LeBihan, Y.-V., & Pawlyn, C. (2025). *Evaluating the impact of CRBN mutations on response to immunomodulatory drugs and novel CRBN binding agents in myeloma*. *Blood*, blood.2024025861. Advance online publication. <https://doi.org/10.1182/blood.2024025861>
- Delvecchio, M., Gaucher, J., Aguilar-Gurrieri, C., Ortega, E., & Panne, D. (2013). Structure of the p300 catalytic core and implications for chromatin targeting and HAT regulation. *Nature Structural and Molecular Biology*, 20(9), 1040–1046. <https://doi.org/10.1038/nsmb.2642>
- Georgopoulos, K., Moore, D. D., & Derfler, B. (1992). Ikaros, an Early Lymphoid-Specific Transcription Factor and a Putative Mediator for T Cell Commitment. *Science*, 258(5083), 808–812. <https://doi.org/10.1126/science.1439790>
- Gooding, S., Ansari-Pour, N., Towfic, F., Ortiz Estévez, M., Estévez, E., Chamberlain, P. P., Tsai, K.-T., Flynt, E., Hirst, M., Rozelle, D., Dhiman, P., Neri, P., Ramasamy, K., Bahlis, N., Vyas, P., & Thakurta, A. (2021). Multiple cereblon genetic changes are associated with acquired resistance to lenalidomide or pomalidomide in multiple myeloma. *Blood*, 137(2), 232–237. <https://doi.org/10.1182/blood.2020007081>
- Hawley, T. S., & Hawley, R. G. (n.d.). Flow Cytometry Protocols Third Edition. In *Methods in Molecular Biology* (Vol. 699). www.springer.com/series/7651

Jones, J. R., Barber, A., Le Bihan, Y. V., Weinhold, N., Ashby, C., Walker, B. A., Wardell, C. P., Wang, H., Kaiser, M. F., Jackson, G. H., Davies, F. E., Chopra, R., Morgan, G. J., & Pawlyn, C. (2021). Mutations in CRBN and other cereblon pathway genes are infrequently associated with acquired resistance to immunomodulatory drugs.

Leukemia, 35(10), 3017–3020. <https://doi.org/10.1038/s41375-021-01373-4>

Joseph, N. S., Kaufman, J. L., Madhav, Dhodapkar, V., Hofmeister, C. C., Almula, D. K., Leonard, Heffner, T., Gupta, V. A., Boise, L. H., Lonial, S., & Nooka, A. K. (2020). Long-Term Follow-Up Results of Lenalidomide, Bortezomib, and Dexamethasone Induction Therapy and Risk-Adapted Maintenance Approach in Newly Diagnosed Multiple Myeloma. In *J Clin Oncol* (Vol. 38). <https://doi.org/10.1200/JCO.19.02515>

Krönke, J., Udeshi, N. D., Narla, A., Grauman, P., Hurst, S. N., McConkey, M., Svinkina, T., Heckl, D., Comer, E., Li, X., Ciarlo, C., Hartman, E., Munshi, N., Schenone, M., Schreiber, S. L., Carr, S. A., & Ebert, B. L. (2014). Lenalidomide causes selective degradation of IKZF1 and IKZF3 in multiple myeloma cells. *Science*, 343(6168), 301–305. <https://doi.org/10.1126/science.1244851>

Kyle, R. A., Larson, D. R., Therneau, T. M., Dispenzieri, A., Kumar, S., Cerhan, J. R., & Rajkumar, S. V. (2018). Long-Term Follow-up of Monoclonal Gammopathy of Undetermined Significance. *New England Journal of Medicine*, 378(3), 241–249. <https://doi.org/10.1056/nejmoa1709974>

Lasko, L. M., Jakob, C. G., Edalji, R. P., Qiu, W., Montgomery, D., Digiammarino, E. L., Hansen, T. M., Risi, R. M., Frey, R., Manaves, V., Shaw, B., Algire, M., Hessler, P., Lam, L. T., Uziel, T., Faivre, E., Ferguson, D., Buchanan, F. G., Martin, R. L., ... Bromberg, K. D. (2017). Discovery of a selective catalytic p300/CBP inhibitor that

targets lineage-specific tumours. *Nature*, 550(7674), 128–132.

<https://doi.org/10.1038/nature24028>

Lu, G., Middleton, R. E., Sun, H., Naniong, M. V., Ott, C. J., Mitsiades, C. S., Wong, K. K., Bradner, J. E., & Kaelin, W. G. (2014). The myeloma drug lenalidomide promotes the cereblon-dependent destruction of ikaros proteins. *Science*, 343(6168), 305–309.

<https://doi.org/10.1126/science.1244917>

Miller, E. (2004). Apoptosis measurement by annexin v staining. *Methods in molecular medicine*, 88, 191–202. <https://doi.org/10.1385/1-59259-406-9:191>

Neri, P., Barwick, B. G., Jung, D., Patton, J. C., Maity, R., Tagoug, I., Stein, C. K., Tilmont, R., Leblay, N., Ahn, S., Lee, H., Welsh, S. J., Riggs, D. L., Stong, N., Flynt, E., Thakurta, A., Keats, J. J., Lonial, S., Bergsagel, P. L., ... Bahlis, N. J. (2024). ETV4-Dependent Transcriptional Plasticity Maintains MYC Expression and Results in IMiD Resistance in Multiple Myeloma. *Blood Cancer Discovery*, 5(1), 56–73.

<https://doi.org/10.1158/2643-3230.BCD-23-0061>

Nicosia, L., Spencer, G. J., Brooks, N., Amaral, F. M. R., Basma, N. J., Chadwick, J. A., Revell, B., Wingelhofer, B., Maiques-Diaz, A., Sinclair, O., Camera, F., Ciceri, F., Wiseman, D. H., Pegg, N., West, W., Knurowski, T., Frese, K., Clegg, K., Campbell, V. L., ... Somervaille, T. C. P. (2023). Therapeutic targeting of EP300/CBP by bromodomain inhibition in hematologic malignancies. *Cancer Cell*, 41(12), 2136–2153.e13. <https://doi.org/10.1016/j.ccell.2023.11.001>

Rajkumar, S. V. (2022). Multiple myeloma: 2022 update on diagnosis, risk stratification, and management. *American Journal of Hematology*, 97(8), 1086–1107.

<https://doi.org/10.1002/ajh.26590>

RRMM: An overview. (2022, June 7). AJMC. <https://www.ajmc.com/view/rrmm-an-overview>

Searle, E., Campbell, V., Pawlyn, C., Bygrave, C., Gooding, S., Cavet, J., Jenner, M. W., Radhakrishnan, V., Knapper, S., el-Sharkawi, D., Knurowski, T., Clegg, K., Henry West, W., Haynes, D., Frese, K., & Somerville, T. (2023). *Tolerability and Clinical Activity of Novel First-In-Class Oral Agent, inobrodib (CCS1477), in Combination With Pomalidomide and Dexamethasone in Relapsed/Refractory Multiple Myeloma*. <https://doi.org/10.1182/blood-2023-174652>

Shaffer, A. L., Emre, N. C. T., Lamy, L., Ngo, V. N., Wright, G., Xiao, W., Powell, J., Dave, S., Yu, X., Zhao, H., Zeng, Y., Chen, B., Epstein, J., & Staudt, L. M. (2008). IRF4 addiction in multiple myeloma. *Nature*, *454*(7201), 226–231. <https://doi.org/10.1038/nature07064>

Steinberger, J., Robert, F., Hallé, M., Williams, D. E., Cencic, R., Sawhney, N., Pelletier, D., Williams, P., Igarashi, Y., Porco, J. A., Rodriguez, A. D., Kopp, B., Bachmann, B., Andersen, R. J., & Pelletier, J. (2019). Tracing MYC Expression for Small Molecule Discovery. *Cell Chemical Biology*, *26*(5), 699-710.e6. <https://doi.org/10.1016/j.chembiol.2019.02.007>

Vannam, R., Sayilgan, J., Ojeda, S., Karakyriakou, B., Hu, E., Kreuzer, J., Morris, R., Herrera Lopez, X. I., Rai, S., Haas, W., Lawrence, M., & Ott, C. J. (2021). Targeted degradation of the enhancer lysine acetyltransferases CBP and p300. *Cell Chemical Biology*, *28*(4), 503-514.e12. <https://doi.org/10.1016/j.chembiol.2020.12.004>

Welsh, S. J., Barwick, B. G., Meermeier, E. W., Riggs, D. L., Shi, C. X., Zhu, Y. X., Sharik, M. E., Du, M. T., Abrego Rocha, L. D., Garbitt, V. M., Stein, C. K., Petit, J. L., Meurice, N., Alvarado, Y. T., Fonseca, R., Todd, K. T., Brown, S., Hammond, Z. J., Cuc, N. H., ...

Bergsagel, P. L. (2024). Transcriptional Heterogeneity Overcomes Super-Enhancer Disrupting Drug Combinations in Multiple Myeloma. *Blood Cancer Discovery*, 5(1), 34–55. <https://doi.org/10.1158/2643-3230.BCD-23-0062>

Yadav, B., Wennerberg, K., Aittokallio, T., & Tang, J. (2015). Searching for Drug Synergy in Complex Dose-Response Landscapes Using an Interaction Potency Model. *Computational and Structural Biotechnology Journal*, 13, 504–513. <https://doi.org/10.1016/j.csbj.2015.09.001>

Zhu, Y. X., Braggio, E., Shi, C. X., Bruins, L. A., Schmidt, J. E., Van Wier, S., Chang, X. B., Bjorklund, C. C., Fonseca, R., Bergsagel, P. L., Orłowski, R. Z., & Stewart, A. K. (2011). Cereblon expression is required for the antimyeloma activity of lenalidomide and pomalidomide. *Blood*, 118(18), 4771–4779. <https://doi.org/10.1182/blood-2011-05-356063>